Chemical Bonding Hot Paper

International Edition: DOI: 10.1002/anie.201503845
German Edition: DOI: 10.1002/ange.201503845

The Nature of Bonding between Argon and Mixed Gold–Silver Trimers**

Armin Shayeghi, Roy L. Johnston, David M. Rayner, Rolf Schäfer, and André Fielicke**

Abstract: *The controversial nature of chemical bonding between noble gases and noble metals is addressed. Experimental evidence of exceptionally strong Au–Ar bonds in Ar complexes of mixed Au–Ag trimers is presented. IR spectra reveal an enormous influence of the attached Ar atoms on vibrational modes, particularly in Au-rich trimers, where Ar atoms are heavily involved owing to a relativistically enhanced covalency. In Ag-rich trimers, vibrational transitions of the metal framework predominate, indicating a pure electrostatic character of the Ag–Ar bonds. The experimental findings are analyzed by means of DFT calculations, which show how the relativistic differences between Au and Ag are manifested in stronger Au–Ar binding energies. Because of the ability to vary composition and charge distribution, the trimers serve as ideal model systems to study the chemical nature of the bonding of noble gases to closed-shell systems containing gold.*

The chemistry of noble gases and noble metals has attracted a great deal of curiosity and broad interest in recent decades.[1] In particular, the discovery of the first isolable compound containing Au–Xe bonds by Seidel and Seppelt in 2000, in the form of the $[AuXe_4]^{2+}$ cation, created significant interest.[2] Subsequently, noble gas (Ng) containing molecules such as NgAuX (Ng = Ne, Ar, Kr; X = Cl, F)[3,4] and $[AuXe_n]^{2+}$ ($n = 1, 2$) were found,[5] further supporting the concept that Ng atoms can directly bind to noble metals, such as gold. It seems the nobleness of the Group 11 and Group 18 elements cannot be taken as face value.

The investigation of closed-shell interactions between Au^+ and Ng atoms began somewhat earlier,[6–8] and is still the subject of numerous studies,[9–12] although Au^+–Ng complexes are putatively simple two-atom systems. Various effects, from dispersion forces and charge-induced dipole interactions up to even a degree of covalency, play an important role in the description of their interesting chemical bonding. In the 1990s, Pyykkö suggested an increased covalency of the Au^+–Ng interaction as the Ng changes from He to Xe, based on a remarkable charge transfer from Xe to Au^+ formally indicating a chemical bond.[6] This proposed increased covalency was questioned and attributed instead to long-range polarization and dispersion effects.[7] However, several subsequent theoretical studies have supported the higher-level calculations by Pyykkö et al.,[13] by questioning the explanation based on higher order multipoles through CCSD-(T) investigations.[10,14] All-electron Dirac–Coulomb CCSD-(T) calculations in the relativistic four-component framework indicate the formation of polar covalent bonds in Au^+–Ng complexes, supporting these suggestions.[11] Another recent CCSD(T) and DFT bond analysis of M–Ng (M = Cu, Ag, Au; Ng = Kr, Xe, Rn) complexes of different charge states also revealed that in cationic Au^+–Ng complexes, both electrostatic and covalent interactions are responsible for the bond strength,[12] while the bonds in anionic and neutral species are of pure electrostatic nature. The results of this study can be explained by relativistic bond length contractions owing to stabilization of s and p shells and destabilization of the d and f shells. These previous and recent studies, however, point to the still-open questions about this unusually strong closed-shell interaction of the d^{10} Au^+ ion with a Ng atom.[8]

To gain further insight into this problem, mixed trimeric clusters of gold and silver can serve as ideal model systems. The closed-shell triangles[15] allow the observation of the dependence of the bond nature on the composition and the asymmetric charge distribution, which is due to the different

[*] A. Shayeghi, Prof. Dr. R. Schäfer
Eduard-Zintl-Institut, Technische Universität Darmstadt
Alarich-Weiss-Strasse 8, 64287 Darmstadt (Germany)
E-mail: shayeghi@cluster.pc.chemie.tu-darmstadt.de
Prof. Dr. R. L. Johnston
School of Chemistry, University of Birmingham
Edgbaston, Birmingham B15 2TT (UK)
Dr. D. M. Rayner
National Research Council of Canada
100 Sussex Drive, Ottawa, Ontario K1A 0R6 (Canada)
Dr. A. Fielicke
Institut für Optik und Atomare Physik, Technische Universität Berlin
Hardenbergstrasse 36, 10623 Berlin (Germany)
E-mail: fielicke@physik.tu-berlin.de

[**] We gratefully acknowledge the support of the Stichting voor Fundamenteel Onderzoek der Materie (FOM) for providing beam time on FELIX, and the FELIX staff for their skilful assistance, in particular Dr. B. Redlich and Dr. A. F. G. van der Meer. This work is supported by the Fritz-Haber Institute of the Max-Planck Society, the Cluster of Excellence "Unifying Concepts in Catalysis" coordinated by the Technical University Berlin and funded by the Deutsche Forschungsgemeinschaft (DFG). We acknowledge financial support by the DFG (grants SCHA 885/10-2 and FI 893/3) and the Merck'sche Gesellschaft für Kunst und Wissenschaft e.V. The calculations reported herein are performed on the following HPC facilities: The University of Birmingham Blue-BEAR facility;[42] the MidPlus Regional Centre of Excellence for Computational Science, Engineering and Mathematics, funded under EPSRC grant EP/K000128/1; and via our membership of the UK's HPC Materials Chemistry Consortium, which is funded by EPSRC (EP/L000202). This work made use of the facilities of ARCHER, the UK's national high-performance computing service, which is funded by the Office of Science and Technology through EPSRC's High End Computing Programme.

Supporting information for this article is available on the WWW under http://dx.doi.org/10.1002/anie.201503845.

Pauling electronegativities of 2.5 and 1.9 for gold and silver, respectively.[16] Such noble metal clusters are chemically very interesting objects,[17] especially owing to their remarkable optical[18,19] and catalytic properties,[20–23] engaging broad interest in Au–Ag nanoalloy clusters.[24]

Here, the study of IR spectra can be of considerable benefit, since vibrational modes sensitively depend on the chemical environment. A common technique to record IR spectra of small and isolated molecules (for example, metal clusters) is messenger-atom far-IR multiple-photon dissociation (FIR-MPD) spectroscopy,[25] where the desorption of Ng atoms attached to the molecules acts as a probe for photon absorption. The weakly bound so-called messenger atoms provide easily detectable dissociation channels without usually influencing the electronic structure of their host molecules considerably. However, it has been previously shown for small and neutral Au clusters tagged with Kr that the Ng does not act as a mere messenger and has to be considered as an integral part of the complex.[26,27] On the other hand, in neutral Ag trimers, the Ng atoms can lead to some band shifts but do not perturb the vibrational spectrum significantly.[28] The covalent character of such neutral M–Ng bonds (M = Be, Cu, Ag, Au, Pt; Ng = He, Ne, Ar, Kr, Xe), to some extent, has also been attributed to non-dispersive and non-covalent weak interactions, similar to the hydrogen bond.[29] But for the closed-shell gold dimer Au_2, a strengthening of the Au–Au bond is observed upon absorbing Kr, resulting in significantly influenced IR spectra, pointing to an increased covalent character.[30] On this basis, the goal of this study is to shed light on the Au^+–Ng closed-shell interaction with the help of Ar complexes of mixed Au–Ag trimer cations by means of experimental IR spectra and DFT calculations.

The general procedure is to compare calculated harmonic IR spectra of the cationic mixed trimer compositions, with and without the inclusion of Ar atoms, to experimental IR spectra. The latter are obtained by FIR-MPD spectroscopy, which has been described in detail elsewhere.[25,31] Briefly, Ar-tagged Au–Ag trimer cations are formed by pulsed laser vaporization of an Au–Ag alloy target, using a mixture of 0.25% Ar in He as the expansion gas. The clusters are thermalized to 150 K by a cryogenic nozzle and detected by reflectron time-of-flight mass spectrometry. An intense and tunable FIR pulse from the free electron laser for infrared experiments (FELIX)[32] irradiates the beam in a counter-propagating fashion. If the IR radiation resonantly couples to a vibrational mode, multiple photons can be absorbed, which heats up the cluster and leads to its dissociation (for example, evaporation of Ng atoms). The mass signal depletion monitored as a function of the FELIX wavelength leads to IR spectra, which are shown on a cross-section scale.[33]

The trimer isomers including Ar atoms are locally optimized using NWChem v6.3,[34] employing the def2-TZVPP basis set and the corresponding scalar relativistic small-core effective core potential (def2-ECP).[35] The long-range corrected xc functional LC-ωPBEh[36] is used, which has been shown to reliably reproduce optical spectra.[37] The higher amount of Hartree–Fock exchange, at long-range, has also been shown to be useful in describing the weaker (non-covalent) M-Ng (M = Cu, Ag, Au; Ng = Kr, Xe, Rn) bond in complexes with small metal clusters.[38] It should be mentioned that the theoretical description of Ng binding energies from DFT calculations is generally uncertain as long-range dispersion interactions are not treated correctly.[39] The relaxed structures are further used in harmonic frequency calculations leading to IR line spectra, which are convoluted with Gaussian functions with a FWHM of 5 cm^{-1} for a better comparison with the experiments.

The mass spectra of the considered molecules reflect an increased strength of the cluster–Ar bond in Au-rich trimers, as highlighted in Figure 1. The signal intensities of Ar-tagged

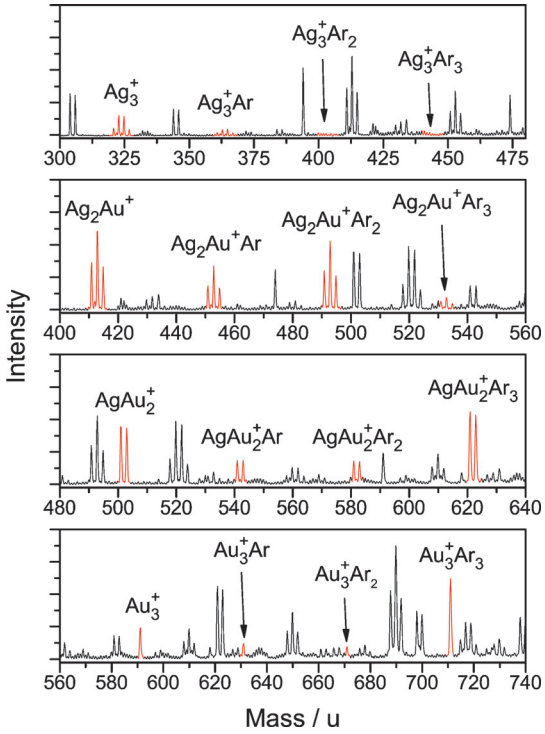

Figure 1. Mass spectrum of $Au_nAg_m^+ \cdot Ar_k$ clusters. The complexes of trimeric clusters with $n+m=3$ and $k=0$–3 are highlighted. Enhancement of intensities of Ar-tagged trimer species are observed with an increasing amount of Au.

species increase with the number of Au atoms in the trimers. The $Au_3^+ \cdot Ar_3$ cluster has a significantly larger intensity than bare Au_3^+, indicating an increased formation in the cluster source. The overall structural motif of the trimeric cations is the triangle with D_{3h} symmetry for Au_3^+ and Ag_3^+ and C_{2v} symmetry for the mixed Au_2Ag^+ and $AuAg_2^+$. Geometries including Ar-tagged species, together with differential binding energies (eV), are shown in Figure 2. For the Au_3^+ cluster, the calculated Ar binding energies for the first, the second, and the third Ar atom are 0.31 eV, 0.28 eV, and 0.26 eV, respectively, which is in good agreement with experimental values from temperature-dependent Ar tagging.[40] Additional calculations for the closed-shell Au^+–Ar complex also verify the validity of the level of theory adopted, as the Au^+–Ar bond length and binding energy are calculated to be 250 pm and 0.48 eV, respectively, which is in excellent agreement with some of the highest-level calculations avail-

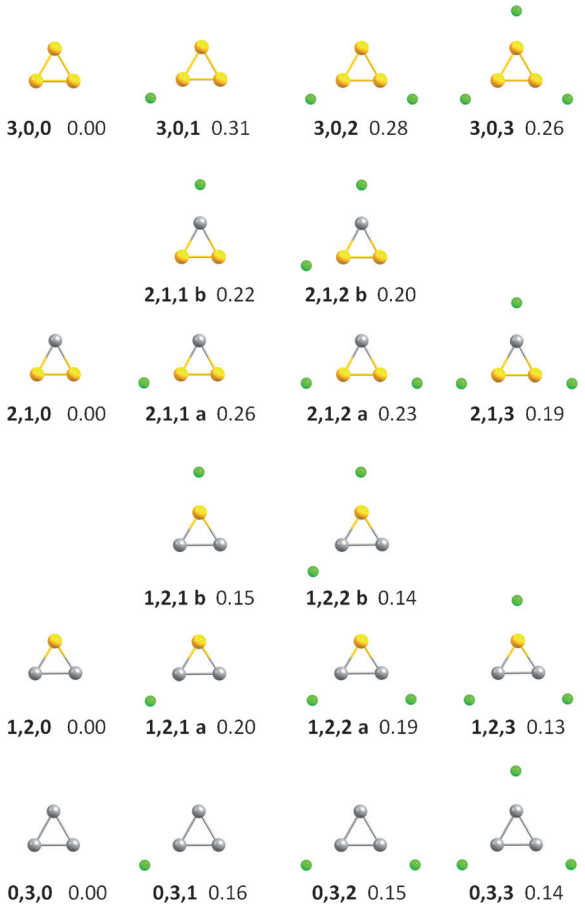

Figure 2. Structures of $Au_3^+{\cdot}Ar_k$, $Au_2Ag^+{\cdot}Ar_k$, $AuAg_2^+{\cdot}Ar_k$, and $Ag_3^+{\cdot}Ar_k$ ($k=1$–3) clusters. The bold numbers represent the *n*,*m*,*k* in $Au_nAg_m^+{\cdot}Ar_k$ followed by the differential Ar binding energies in eV. Out-of-plane isomers are less stable and therefore not shown here.

able.[11,14,41] The differential binding energies show a decreasing trend, depending on the number of Ar atoms as well as the composition, which means doping the Au_3^+ cluster with Ag atoms reduces the binding energies.

The experimental FIR-MPD spectra for the trimeric cations, with each metal atom coordinated by an Ar atom, are presented in Figure 3. Ar complexes of the Ag_3^+ cluster were not abundant under the given experimental conditions and are therefore not included. When Ar acts as a messenger ligand, normal modes with significant Ar displacements are typically below 100 cm^{-1}. In the case of the $Au_3^+{\cdot}Ar_3$ cluster, the main vibrational transition calculated at 134 cm^{-1}, consisting of two degenerate modes, is in excellent agreement with the FIR-MPD spectrum. The same conclusion can be drawn for the $Au_2Ag^+{\cdot}Ar_3$ cluster, where the calculations fit the experimental spectrum particularly well. In contrast, the calculated harmonic modes of $AuAg_2^+{\cdot}Ar_3$ are marginally red-shifted (5 cm^{-1}) compared to the measured spectrum. Presumably, the weaker Ag–Ar bond with increased dipolar and dispersive character, when compared to Au–Ar bonds, is responsible for the disagreement in force constants in the DFT calculations.

The calculated vibrational spectra of the bare trimeric cations are also shown in all plots, as dashed gray lines.

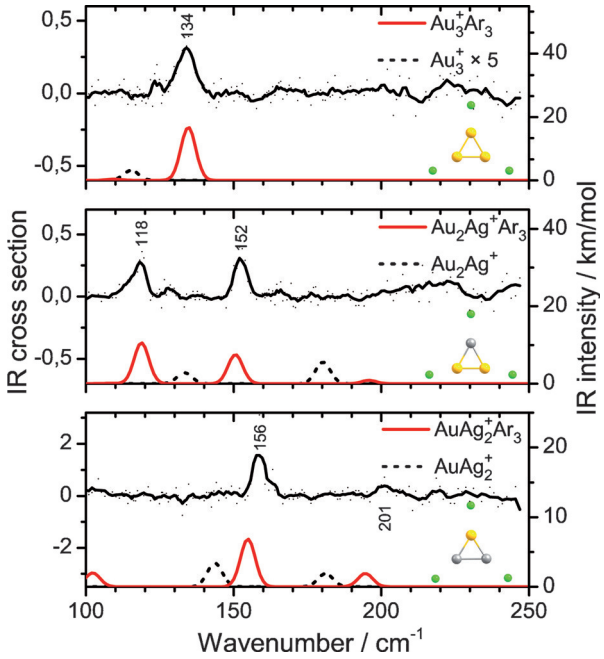

Figure 3. FIR-MPD data points of $Au_nAg_m^+{\cdot}Ar_3$ ($n+m=3$) clusters with a five-point running average as a guide to the eye compared to harmonic IR spectra at the LC-ωPBEh/def2-TZVPP level of theory. Spectra of the respective bare isomers are also shown (dashed gray lines). Experimental peak positions are given in cm^{-1} and are estimated to have an uncertainty of ± 2 cm^{-1}.

Interestingly, bare Au_3^+ does not show the intense mode at 134 cm^{-1} found for the $Au_3^+{\cdot}Ar_3$ complex. Only a low intensity mode at 115 cm^{-1} appears. Adding one Ag atom changes the situation, but still the harmonic IR spectrum of the bare Au_2Ag^+ cluster is significantly different from both experimental and calculated spectra of the $Au_2Ag^+{\cdot}Ar_3$ complex. For the Ag-rich $AuAg_2^+$ cluster, the harmonic IR spectrum shows a better correspondence with the experimental spectrum of $AuAg_2^+{\cdot}Ar_3$, which is simply red-shifted by about 10 cm^{-1} and of lower IR intensity for the dominating mode at around 150 cm^{-1}.

In the singly Ar-tagged **2,1,1** and **1,2,1** and in the doubly Ar-tagged **2,1,2** and **1,2,2** the calculations show that Ar positions, where the metal atoms have one homonuclear and one heteronuclear bond, are preferred over positions with two heteronuclear bonds. This is independent from the larger partial charge on the Ag atoms, as obtained from both Löwdin and Mulliken population analyses (Table 1). As expected, the larger partial charge is located on the Ag atoms, causing their positions to show the strongest ion-induced dipole interactions with Ar atoms. Apparently, ion-induced dipole inter-

Table 1: Partial charges from population analyses employing the Löwdin and the Mulliken (in parantheses) method for the bare mixed trimeric cations.

Center	Au_2Ag^+	$AuAg_2^+$
Au	0.30 (0.14)	0.24 (0.00)
Ag	0.40 (0.72)	0.38 (0.50)

actions are not the main part of the interplay which controls the Ar attachment in cationic mixed Au–Ag clusters.

This behavior may be interpreted in terms of the relativistically enhanced ionization energy of Au, leading to a higher electronegativity and a stronger covalent character of the Au^+–Ar bond as predicted by Pyykkö,[6] since, when comparing pure Au_3^+ and Ag_3^+ clusters, the total Ar binding energy for $Au_3^+{\cdot}Ar_3$ (0.84 eV) is significantly larger than for $Ag_3^+{\cdot}Ar_3$ (0.45 eV). The increased binding energies in Au-rich clusters do not result from charge distribution effects, as can be seen for the D_{3h} symmetric pure clusters. Also, they cannot be caused by differences in isotropic dipole polarizabilities α_{iso}. From the independent components of the polarizability tensor, $\alpha_{iso} = 3.6$ Å^3/atom for Au_3^+, while it is slightly increased to 3.8 Å^3/atom for Ag_3^+. Thus, neither partial charges nor polarizabilities can explain the stronger Ar binding in Au-rich clusters, so this effect must be related to the stronger covalent component of the Au^+–Ar bond caused by the larger electronegativity of Au, which is a pure relativistic effect.[6,16]

The increased stabilities are reflected in bond lengths as well, which can be found in Table 2 for triply tagged trimers of all compositions. Here, the Au–Ar bond length in $Au_3^+{\cdot}Ar_3$ (259 pm) is even shorter than the Au–Au bond (261 pm). In the $Ag_3^+{\cdot}Ar_3$ cluster, however, the Ag–Ag bond (267 pm) is somewhat shorter than the Ag–Ar bond (277 pm). In the silver-rich composition $AuAg_2^+{\cdot}Ar_3$, the Au–Ar bond length is increased to 279 pm. This lengthening refers to a stronger electrostatic character due to a strong charge transfer from the two Ag atoms to the Au atom, while the the Au–Ar bond length in the gold-rich composition $Au_2Ag^+{\cdot}Ar_3$ is 263 pm.

Table 2: Lengths (in pm) of the M–Ar and M–M (M = Au, Ag) bonds in the triply Ar-tagged trimeric cations.

Bond	$Au_3^+{\cdot}Ar_3$	$Au_2Ag^+{\cdot}Ar_3$	$AuAg_2^+{\cdot}Ar_3$	$Ag_3^+{\cdot}Ar_3$
Au–Au	261	255	–	–
Au–Ar	259	263	279	–
Au–Ag	–	268	261	–
Ag–Ar	–	268	270	277
Ag–Ag	–	–	277	267

Further insight can be obtained from the evolution of the IR spectra with the number of Ar atoms. Harmonic IR spectra of all trimer compositions and their Ar species (including $Ag_3^+{\cdot}Ar_k$) are presented in Figure 4. Additionally, vibrational displacements for significant intensities of triply tagged $Au_nAg_m^+{\cdot}Ar_3$ species are visualized. The IR spectra of the $Ag_3^+{\cdot}Ar_k$ cluster (bottom line) do not show a strong influence of the attached Ar atoms. Changing the symmetry from D_{3h} to C_{2v}, by Ar attachment leading to **0,3,1** and **0,3,2**, causes the degenerate symmetric and non-symmetric stretching modes at 122 cm^{-1} to split. Additionally, the dipole-forbidden breathing mode at 180 cm^{-1} gains a non-zero transition dipole moment. In the $Ag_3^+{\cdot}Ar_3$ cluster (**0,3,3**), the breathing mode disappears and again two degenerate stretching modes remain, which are minutely shifted by 7 cm^{-1} compared to bare Ag_3^+. A similar situation is found for the $AuAg_2^+$ cluster, where the normal modes are barely influ-

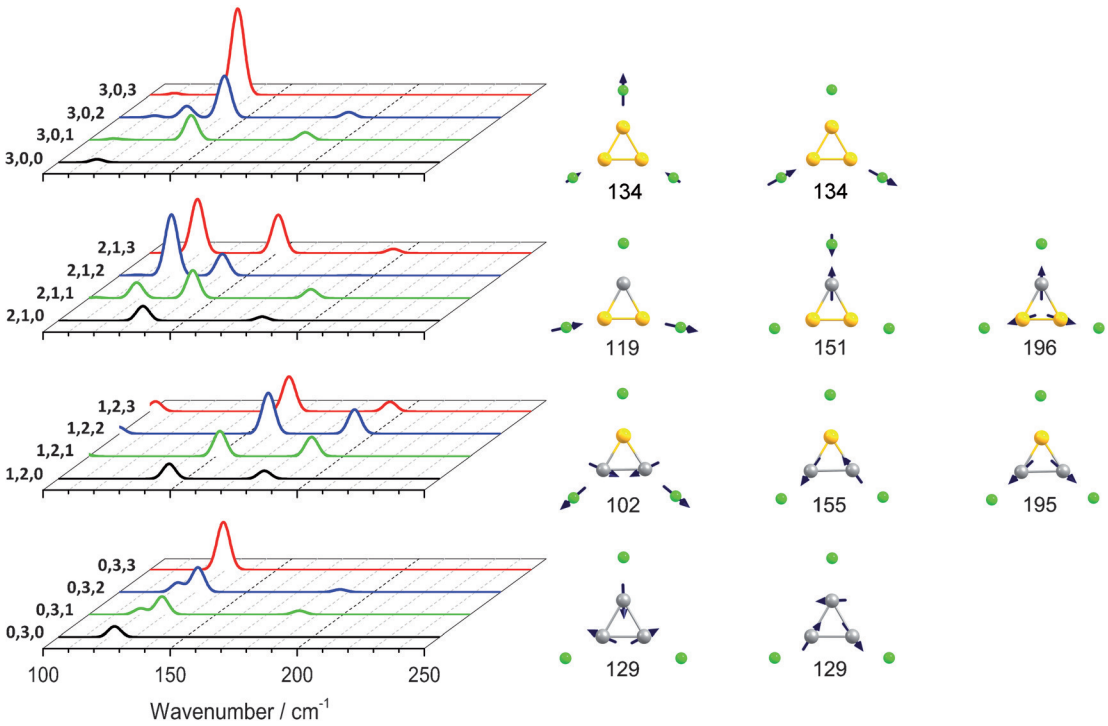

Figure 4. Evolution of harmonic infrared spectra of all trimer compositions with the number of attached Ar atoms (on the left). The vibrational displacement for the modes with significant intensities are shown for the energetically lowest-lying triply tagged trimers (on the right, cm^{-1}). While the spectra of the Ag-rich compositions are only minutely changed by the Ar atoms, Au-rich clusters are more strongly affected depending on the number of attached Ar atoms, and the Ar atoms are heavily involved in vibrations.

enced by the messenger atom. The only deviations are slight shifts (that is, the symmetric stretching mode undergoes a blue-shift with increasing Ar attachment) and minute changes in intensities. For Au_2Ag^+, which is an Au-rich composition, the situation appears quite different. Several symmetric and non-symmetric Ar stretching modes are now involved in the considered frequency range. This effect continues in the $Au_3^+{\cdot}Ar_k$ cluster, where the Ar attachment dramatically influences the normal modes and becomes particularly clear when comparing bare Au_3^+ and the $Au_3^+{\cdot}Ar_3$ cluster. While Au_3^+ only shows two degenerate stretching modes at 115 cm^{-1} in the considered frequency range, in $Au_3^+{\cdot}Ar_3$ two degenerate high intensity modes additionally appear at 134 cm^{-1}, where the Ar atoms are strongly involved. These observations reveal a tremendous influence of the Ng atom on the IR spectra and the binding energies in Au-rich trimers, which must be due to the relativistic differences between Au and Ag. Furthermore, this effect is expected to increase when heavier Ng atoms are attached, owing to their larger polarizability, donating more electron density to the electronegative Au atom.[6]

In conclusion, harmonic IR spectra from DFT calculations in conjunction with the experimental FIR-MPD spectra have provided an approach for understanding further the intriguing Au^+–Ng interaction by investigating Ar bonds to partially positively charged Au atoms in the mixed Au-Ag trimers. Binding energies of the Ar atoms indicate strong bonds in the Au-rich species, while it has been shown that Ag-rich clusters are negligibly affected by Ar atoms and behave like the unperturbed clusters being surrounded by weakly bound messenger atoms. For the Au-rich compositions, Ar atoms are involved in the transitions and the tagged clusters show molecule-like vibrational modes, which are different from normal modes of the bare cluster, acting like a six-atom molecule. Thus, the Ng atoms can only to some extent be described as mere messengers. Here the actual probe (messenger) acts more like a modifier, which has been interpreted in terms of covalent interactions, charge transfer effects, and ion-induced dipole interactions. In Au-rich clusters, the covalent character of the bonds to Ar atoms is enhanced owing to the high electronegativity of Au, reflecting relativistic effects, while in Ag-rich clusters charge-transfer from the Ag to Au atoms suppresses the donation of electron density from Ar to Au atoms, weakening the covalent character.

Keywords: chemical bonding · clusters · IR spectroscopy · noble gases · noble metals

How to cite: *Angew. Chem. Int. Ed.* **2015**, *54*, 10675–10680
Angew. Chem. **2015**, *127*, 10822–10827

[1] W. Grochala, *Chem. Soc. Rev.* **2007**, *36*, 1632–1655.
[2] S. Seidel, K. Seppelt, *Science* **2000**, *290*, 117–118.
[3] C. J. Evans, A. Lesarri, M. C. L. Gerry, *J. Am. Chem. Soc.* **2000**, *122*, 6100–6105.
[4] X. Wang, L. Andrews, K. Willmann, F. Brosi, S. Riedel, *Angew. Chem. Int. Ed.* **2012**, *51*, 10628–10632; *Angew. Chem.* **2012**, *124*, 10780–10784.
[5] T. Drews, S. Seidel, K. Seppelt, *Angew. Chem. Int. Ed.* **2002**, *41*, 454–456; *Angew. Chem.* **2002**, *114*, 470–473.
[6] P. Pyykkö, *J. Am. Chem. Soc.* **1995**, *117*, 2067–2070.
[7] J. P. Read, A. D. Buckingham, *J. Am. Chem. Soc.* **1997**, *119*, 9010–9013.
[8] R. Wesendrup, P. Schwerdtfeger, *Angew. Chem. Int. Ed.* **2000**, *39*, 907–910; *Angew. Chem.* **2000**, *112*, 938–942.
[9] D. Bellert, W. H. Breckenridge, *Chem. Rev.* **2002**, *102*, 1595–1622.
[10] T. Zeng, M. Klobukowski, *J. Phys. Chem. A* **2008**, *112*, 5236–5242.
[11] L. Belpassi, I. Infante, F. Tarantelli, L. Visscher, *J. Am. Chem. Soc.* **2008**, *130*, 1048–1060.
[12] Z. Jamshidi, K. Eskandari, S. M. Azami, *Int. J. Quantum Chem.* **2013**, *113*, 1981–1991.
[13] D. Schröder, H. Schwarz, J. Hrusak, P. Pyykkö, *Inorg. Chem.* **1998**, *37*, 624–632.
[14] W. H. Breckenridge, V. L. Ayles, T. G. Wright, *J. Phys. Chem. A* **2008**, *112*, 4209–4214.
[15] P. Weis, O. Welz, E. Vollmer, M. M. Kappes, *J. Chem. Phys.* **2004**, *120*, 677–684.
[16] P. Schwerdtfeger, *Chem. Phys. Lett.* **1991**, *183*, 457–463.
[17] P. Pyykkö, *Angew. Chem. Int. Ed.* **2004**, *43*, 4412–4456; *Angew. Chem.* **2004**, *116*, 4512–4557.
[18] O. M. Bakr, V. Amendola, C. M. Aikens, W. Wenseleers, R. Li, L. Dal Negro, G. C. Schatz, F. Stellacci, *Angew. Chem. Int. Ed.* **2009**, *48*, 5921–5926; *Angew. Chem.* **2009**, *121*, 6035–6040.
[19] S. Wang, X. Meng, A. Das, T. Li, Y. Song, T. Cao, X. Zhu, M. Zhu, R. Jin, *Angew. Chem. Int. Ed.* **2014**, *53*, 2376–2380; *Angew. Chem.* **2014**, *126*, 2408–2412.
[20] P. Schwerdtfeger, *Angew. Chem. Int. Ed.* **2003**, *42*, 1892–1895; *Angew. Chem.* **2003**, *115*, 1936–1939.
[21] H. Häkkinen, S. Abbet, A. Sanchez, U. Heiz, U. Landman, *Angew. Chem. Int. Ed.* **2003**, *42*, 1297–1300; *Angew. Chem.* **2003**, *115*, 1335–1338.
[22] P. Gruene, D. M. Rayner, B. Redlich, A. F. van der Meer, J. T. Lyon, G. Meijer, A. Fielicke, *Science* **2008**, *321*, 674–676.
[23] A. P. Woodham, A. Fielicke, *Angew. Chem. Int. Ed.* **2014**, *53*, 6554–6557; *Angew. Chem.* **2014**, *126*, 6672–6675.
[24] R. Ferrando, J. Jellinek, R. L. Johnston, *Chem. Rev.* **2008**, *108*, 845–910.
[25] A. Fielicke, A. Kirilyuk, C. Ratsch, J. Behler, M. Scheffler, G. von Helden, G. Meijer, *Phys. Rev. Lett.* **2004**, *93*, 023401.
[26] L. M. Ghiringhelli, P. Gruene, J. T. Lyon, D. M. Rayner, G. Meijer, A. Fielicke, M. Scheffler, *New J. Phys.* **2013**, *15*, 083003.
[27] L. A. Mancera, D. M. Benoit, *J. Phys. Chem. A* **2015**, *119*, 3075–3088.
[28] A. Fielicke, I. Rabin, G. Meijer, *J. Phys. Chem. A* **2006**, *110*, 8060–8063.
[29] W. Zou, D. Nori-Shargh, J. E. Boggs, *J. Phys. Chem. A* **2013**, *117*, 207–212.
[30] L. M. Ghiringhelli, S. V. Levchenko, *Inorg. Chem. Commun.* **2015**, *55*, 153–156.
[31] A. Fielicke, G. von Helden, G. Meijer, *Eur. Phys. J. D* **2005**, *34*, 83–88.
[32] D. Oepts, A. F. G. van der Meer, P. W. van Amersfoort, *Infrared Phys. Technol.* **1995**, *36*, 297–308.
[33] M. Savoca, J. Langer, D. J. Harding, D. Palagin, K. Reuter, O. Dopfer, A. Fielicke, *J. Chem. Phys.* **2014**, *141*, 104313.
[34] M. Valiev, E. J. Bylaska, N. Govind, K. Kowalski, T. P. Straatsma, H. J. J. Van Dam, D. Wang, J. Nieplocha, E. Apra, T. L. Windus, W. A. de Jong, *Comput. Phys. Commun.* **2010**, *181*, 1477–1489.
[35] F. Weigend, R. Ahlrichs, *Phys. Chem. Chem. Phys.* **2005**, *7*, 3297–3305.
[36] M. A. Rohrdanz, K. M. Martins, J. M. Herbert, *J. Chem. Phys.* **2009**, *130*, 054112–8.

[37] A. Shayeghi, C. J. Heard, R. L. Johnston, R. Schäfer, *J. Chem. Phys.* **2014**, *140*, 054312.
[38] Z. Jamshidi, M. F. Far, A. Maghari, *J. Phys. Chem. A* **2012**, *116*, 12510–7.
[39] S. Grimme, *Wiley Interdiscip. Rev. Comput. Mol. Sci.* **2011**, *1*, 211–228.
[40] S. M. Lang, P. Claes, N. T. Cuong, M. T. Nguyen, P. Lievens, E. Janssens, *J. Chem. Phys.* **2011**, *135*, 224305.
[41] P. Zhang, Y. Zhao, F. Hao, X. Song, G. Zhang, Y. Wang, *J. Mol. Struct. THEOCHEM* **2009**, *899*, 111–116.
[42] See http://www.bear.bham.ac.uk/bluebear for a description of the Blue-BEAR HPC facility.

Received: April 27, 2015
Published online: July 17, 2015

